Phase relations between dynamic lateral earth pressures and acceleration of retaining walls

Abouzar Sadrekarimi
The University of Western Ontario, London, Ontario, Canada

ABSTRACT
Phase differences among seismic earth pressure fluctuations acting on different elevations of a retaining wall and wall acceleration are important in pseudo-static computational methods. In this paper these phase relations are examined through 6 shaking table tests on model retaining walls. Wall acceleration and the fluctuations of dynamic lateral earth pressures on two different elevations of the wall are compared. Comparisons show that the phase difference between the acceleration of the wall and the dynamic lateral earth pressure fluctuations depends on wall acceleration. Such behaviour would cause a wall to either rock or move uniformly back-and-forth during earthquake shaking.

RÉSUMÉ
Les différences de phase entre les fluctuations de pression des terres sismiquesagissant sur des hauteurs différentes d'un mur de soutènement et d'accélération mursont importants dans pseudo-statique des méthodes de calcul. Dans cet article, cesrelations de phases sont examinées à 6 essais sur table vibrante sur les murs de soutènement modèle. Wall accélération et les fluctuations de la dynamique des pressions latérales des terres sur deux niveaux différents de la paroi sont comparées.Les comparaisons montrent que la différence de phase entre l'accélération de la paroilatérale et la dynamique des fluctuations de pression de terre dépend de l'accélérationmur. Un tel comportement serait de provoquer un mur de roche ou de déplacer de manière uniforme de va-et-vient lors de secousses sismiques.

1 INTRODUCTION

Increasing lateral earth pressures on retaining walls during earthquakes has been one of the major causes of their damage and excessive displacement (Seed and Whitman, 1970; Pitilakis and Moutsakis 1989; Dakoulas and Gazetas 2008). Therefore, correct estimation of the active earth pressure distribution acting on retaining walls during earthquakes is vital for evaluating the safety and designing of the wall. Some simplified approaches have been proposed to calculate the rather complicated dynamic earth pressures on retaining walls during earthquakes (Okabe 1924; Mononobe and Matsuo 1929; Wood 1973; Steedman and Zeng 1990; Richards et al. 1999; Choudhury and Singh 2006; Ghosh 2008). Okabe (1924) and Mononobe and Matsuo (1929) extended Coulomb's theory and considered seismic forces by applying earthquake loads as uniform coefficients of the weight of the active failure wedge. This pseudo-static method (known as the Mononobe-Okabe method) has been widely used in practical applications (Mylonakis et al. 2007) and is recommended by several building codes and guidelines (e.g. EAU 1996; FHWA 1997; CHBDC 1998; ASCE 4-98 2000; FEMA 369 2000; PIANC 2001; EN 1997 2002; AASHTO 2006; IBC 2006) because of its simplicity in practical applications and reasonable predictions of the actual dynamic pressures acting on walls (Ishii et al. 1960; Seed and Whitman 1970; Sherif et al. 1982; Whitman 1990; Ebeling et al. 1992; Veletsos and Younan 1994; Dakoulas and Gazetas 2008). However, the phase relations between the lateral earth pressures and wall movement are still debated among investigators (Steedman and Zeng 1990; Kazama and Inatomi 1993; Ting 1993; Zeng 1998; Kim et al. 2004; Lee 2005; Nakamura 2006; Al Atik and Sitar 2008; Choudhury and Ahmad 2008) and are not taken into account by the Mononobe-Okabe method. For example, Ishii et al. (1960) conducted shaking table tests on walls backfilled with sand and observed phase differences as much as 180^{o} between the motion of the wall and the measured lateral pressures. Theoretical analysis and field tests of Tajimi (1973) showed the earth pressure distribution on a retaining wall and the variations of the vibration phase along the wall depend on the shear wave velocity of the backfill. The gravity wall tests of Sherif et al. (1982) showed that the maximum earth force occurred at the time of peak acceleration towards the backfill. Sherif and Fang (1984a, b) did shaking table tests on model rigid walls rotating about their base, and rotating about their top. For the walls rotating about their base they observed that during shaking as the input acceleration was increased the non-linearity of the lateral stress distribution also increased and large lateral stresses developed near top of the wall. They attributed this to the smaller strength of the sand near the surface of the backfill and hence its larger lateral stress transmission characteristic. As a result, the point of application of the total dynamic thrust was observed to rise with increasing the input acceleration. For the walls rotating about their top, dynamic lateral pressures near the top of the wall increased with increasing acceleration and this was attributed to soil arching and those at the bottom of the wall were nearly zero. The point of application of the total dynamic thrust was observed to rise from one-thirds of wall height to 0.55 of wall height when the active state was established. On the other hand, Andersen et al. (1987) conducted shaking table centrifuge model tests on tilting gravity walls and showed that the maximum lateral earth force occurred when the wall moved back against the backfill and the acceleration was maximum in the outward direction.

Through 1g shaking table tests on rigid caisson model walls, Kazama and Inatomi (1993) observed that the dynamic earth pressure distribution followed the trend of

the relative displacement between the backfill and the caisson and there was a phase difference between the inertia force of the caisson and the resultant force of the dynamic earth pressure. Ting (1993) studied the behaviour of waterfront retaining structures during earthquakes and the phase relations between the ground acceleration and the dynamic earth and water thrusts by performing a series of dynamic centrifuge tests. The centrifuge tests involved a model retaining wall, hinged at the base and designed to yield when the total load exceeded the shear resistance of a slider. He found that the Mononobe-Okabe and Westergaard methods were not applicable for estimating the dynamic thrusts from the soil skeleton and pore water, mainly because of the complicated interaction between the retaining wall and the backfill soil. Watanabe et al. (1999) performed shaking table tests on model retaining walls and found that when the shaking acceleration was weak (< 0.3g), acceleration and the dynamic earth pressure were out of phase, and as the shaking became stronger (> 0.4g), they became in phase with each other. Using centrifuge model tests on gravity retaining walls, Nakamura (2006) found significant difference in acceleration of the retaining wall and the backfill, indicating time lag and phase difference between the dynamic earth pressures and inertial forces of the wall. More recently, Al Atik and Sitar (2008) studied the seismic behaviour of cantilever retaining walls in dynamic centrifuge model experiments and found that the dynamic earth pressures and inertial forces did not act at the same time.

In this paper the phase relation between the dynamic lateral earth pressures and the acceleration of a wall is studied using shaking table tests on reduced scale physical models of retaining walls and the implications of the phase difference on the Mononobe-Okabe method are discussed.

2 PHYSICAL MODELING

Results from the 1g shaking table physical model experiments on reduced scale broken-back quay walls performed by the author (Sadrekarimi 2004) are used in this study. Despite some limitations (e.g. reduced stresses, boundary conditions, input motions), 1g shaking table tests can provide useful information on the principal features of soil dynamic behaviour, and thus are useful for the calibration of numerical and analytical methods in geotechnical engineering practice.

2.1 Model Specification

Figure 1 shows the cross section of the broken-back model retaining wall. The model wall is made of concrete (unit weight of 24 kN/m^3) blocks of 4 cm tall and 4 cm wide with varying lengths as shown in Figure 1. A concrete cap (block number 11) of 6 cm tall and 44 cm wide was placed on top of the wall and as a result the total height of the wall became 44 cm. The width of the model wall measured 11.2 cm at the top and 22.5 cm at the bottom. As shown in Figure 1, shear keys (0.45 cm tall and 1 cm long) were implemented on top and bottom surfaces of each concrete block in order to prevent relative displacement between them and preserve the structural integrity of the wall.

Miniature total pressure (E), pore water pressure (P), and acceleration (A) transducers were installed along the centerline of the wall in order to reduce the effect of any sidewall friction of the soil container. Wall lateral displacements and settlement were also measured, however as they are not used in this discussion they are not presented here. A dynamic data logger was used to record and transfer data to a personal computer. A silica sand with specific gravity of sand particles (G_S) = 2.658, maximum void ratio (e_{max}) = 0.943, minimum void ratio (e_{min}) = 0.603, and D_{50} = 0.3 mm was used as the subsoil beneath the model walls. As liquefaction was not the subject of this study, it was prevented by using a very coarse limestone backfill (e_{max} = 0.960, e_{min} = 0.670, D_{50} = 12 mm, and a hydraulic conductivity of 0.5 m/s) behind the walls and a subsoil (seabed) sand relative density of 90%.

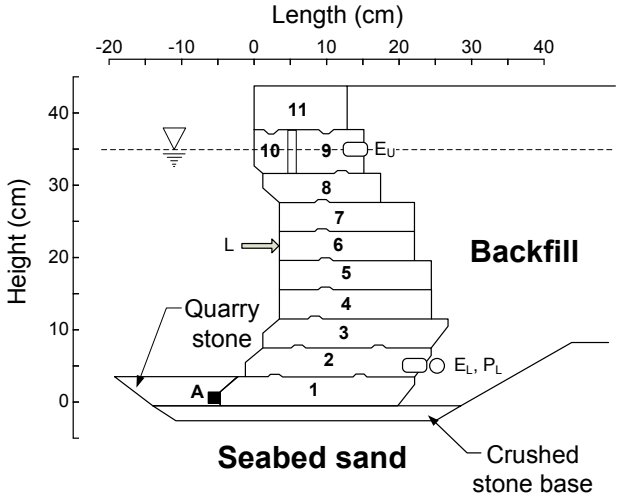

Figure 1. Model section and instrumentations (E_U & E_L: upper and lower Earth pressure transducers, respectively; P_L: lower pore water pressure transducer; A: Accelerometer)

2.2 Model Preparation

The Plexiglas model container measured 180 cm long, 45 cm wide, and 70 cm high and was equipped with carbon dioxide and water inlets and outlets. As the models were intended to simulate a plane strain condition, the main concern was to avoid side effects of the test container. The frictional shear stress between the side walls of the container (parallel to axis of the one-dimensional shaking) and the model was minimized by lubricating (with a thin layer of silicon grease) the Plexiglas sides of the container before each test. As the ratio of the backfill length (≈ 100 cm) to wall height (44 cm) was sufficiently large (> 2), it was assumed that the far end boundaries of the model container would not have any significant effect on the model wall response (Dewoolkar et al. 2001). In addition, an energy absorbing material (Coe et al. 1985; Zeng 1998) was glued to the end walls in order to reduce

energy reflected from the end boundaries and the generation of compression waves.

The subsoil sand was moist tamped to a relative density of 90% following the undercompation method (Ladd 1978) in order to have a uniform density. After completing the subsoil, the concrete wall was placed on the sand and the backfill was poured in the container behind the wall. Using the same pluviation method and drop height a uniform relative density of 52% was produced in the backfill of the model tests. Similar to sand specimen saturation procedure in undrained triaxial testing (Lacasse and Berre 1988), in order to ensure better saturation of the model with water, carbon dioxide gas was circulated through the model from the lower inlet followed by water.

2.3 Testing Procedure

Horizontal sinusoidal excitations with a constant frequency of 2.8 Hz, but different maximum acceleration amplitudes (shown in Figs. 2-7) were applied in the model tests. The constant frequency of 2.8 Hz would correspond to an earthquake predominant frequency of 0.8 Hz (Ortiz et al. 1983) for a 6 m tall prototype wall (i.e. geometrical scaling factor of 14) that falls in the lower range of predominant frequencies of real earthquake motions. For example, the 1992 Petrolia/Cape Mendocino earthquake, 1989 Loma Prieta earthquake at Yerba Buena Island (COSMOS 2010), and the 1936 to 1963 Vrancea earthquakes at Bucharest seismic station (Mandrescu et al. 2002), all had predominant frequencies in the range of 0.7 to 0.8 Hz. The natural frequency of the retaining walls tested in this study is roughly estimated as $20/H^{0.75}$ (IBC 2006), in which H is the height of the wall in meters and f is the natural frequency in Hertz. Using H = 44 cm (see Fig. 1), a natural frequency of 37 Hz is obtained that is considerably larger than the frequency of the input motion applied in these model tests (2.8 Hz) and the applied shaking would not resonate the model; therefore pseudo-static methods are applicable for the determination of lateral earth pressures (Zeng and Steedman 1993).

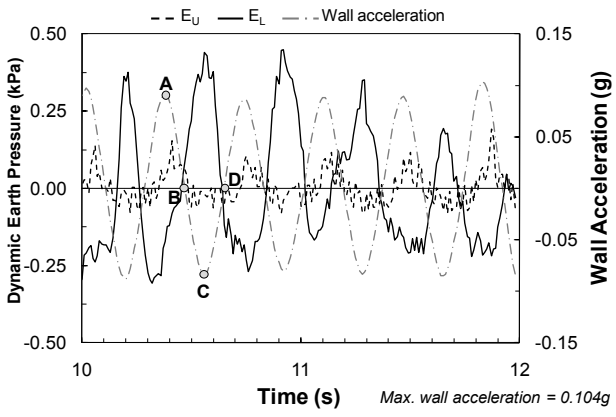

Figure 2. Wall acceleration and dynamic lateral earth pressures (max. wall acceleration = 0.104g)

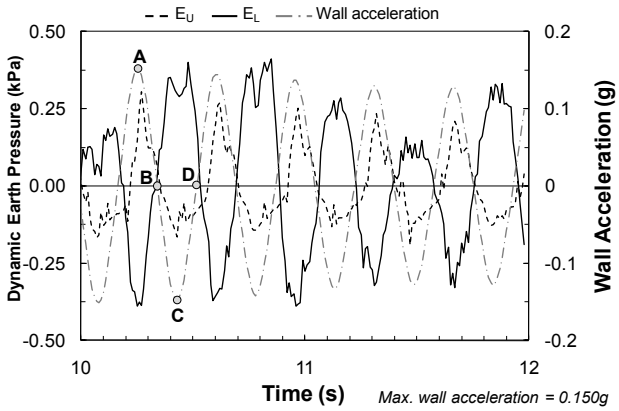

Figure 3. Wall acceleration and dynamic lateral earth pressures (max. wall acceleration = 0.150g)

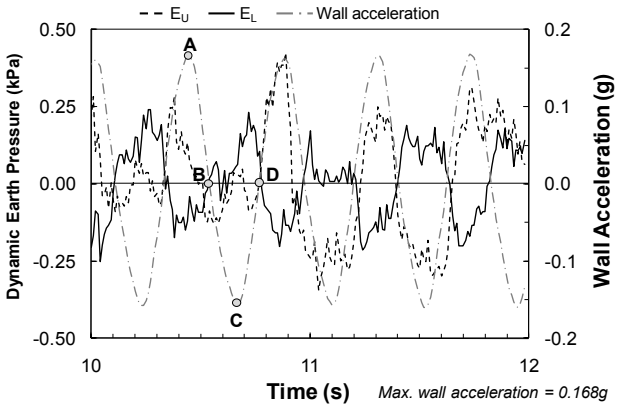

Figure 4. Wall acceleration and dynamic lateral earth pressures (max. wall acceleration = 0.168g)

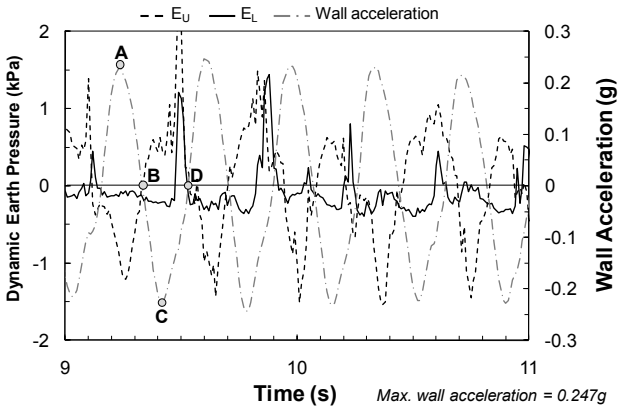

Figure 5. Wall acceleration and dynamic lateral earth pressures (max. wall acceleration = 0.247g)

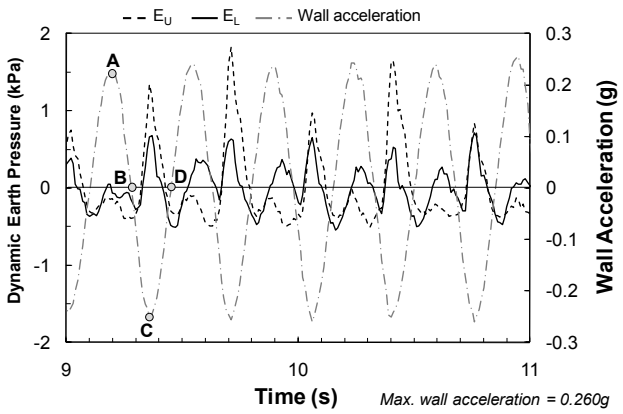

Figure 6. Wall acceleration and dynamic lateral earth pressures (max. wall acceleration = 0.260g)

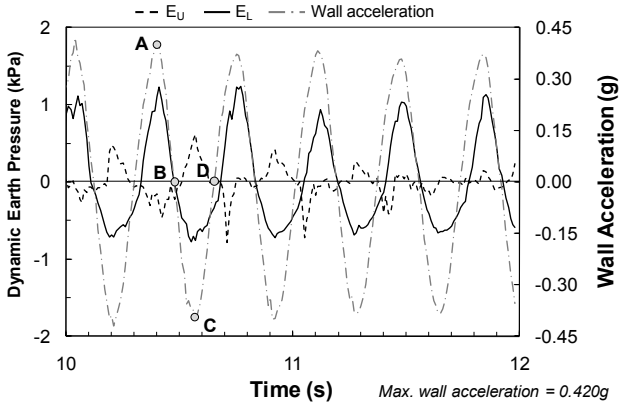

Figure 7. Wall acceleration and dynamic lateral earth pressures (max. wall acceleration = 0.420g)

3 RESULTS AND DISCUSSIONS

Effective lateral earth pressure was measured at the upper elevation of the wall, while at the lower elevation it was calculated by deducting the pore water pressure (P_L) from the total lateral earth pressure and the oscillations of these pressures were taken as the dynamic effective lateral earth pressures (E_L and E_U). Time histories of the dynamic effective lateral earth pressures at the upper (E_U) and lower (E_L) elevations of the walls and the acceleration time history recorded at the toe of the walls are shown in Figures 2 to 7. In these figures, points A, B, C, and D show a full cycle (complete period) of walls motion. Points A and C indicate instances at which wall acceleration reaches maximum in forward (away from backfill) and backward (towards backfill) directions, respectively and points B and D show moments at which wall acceleration becomes zero. Note that the more complex frequency content of the dynamic lateral earth pressures is likely because of the complicated wall-backfill-subsoil interaction response.

At relatively small wall accelerations (< 0.200g in Figures 2, 3 and 4), dynamic lateral earth pressures at E_U and E_L act almost completely out-of-phase. When the wall accelerates forward (positive wall accelerations), E_U increases to a maximum while E_L decreases to a minimum. This indicates that at the upper elevation of the wall (E_U), the backfill soil accelerates forward faster than the wall, because of the very small effective stress has better lateral stress transmission characteristics, and likely reaches an active state (fails) whereas at the lower elevation (E_L), the backfill soil accelerates forward slower than the wall (i.e. the induced inertia force moves the wall forwards more than the backfill soil, leading to the reduced earth pressure). In this case, E_U varies in-phase with wall acceleration (or out of phase with wall inertia) but E_L changes out-of-phase with wall acceleration indicating a rocking type wall motion. As wall acceleration drops to zero (A to B), E_U and E_L decrease and increase towards zero, respectively. When the wall accelerates backwards from B to C, E_U drops (walls backward acceleration is smaller than that of the backfill) and E_L increases (walls backward acceleration is larger than that of the backfill) to a maximum value (point C) at which a passive state is likely reached and the backfill and the wall collide. Finally, as wall acceleration reduces to zero again (C to D), both E_U and E_L reduce to zero and the wall and backfill move at same accelerations.

At intermediate levels of wall acceleration (Figures 5 and 6), the dynamic lateral earth pressures at E_U and E_L fluctuate more-or-less in-phase. While the wall accelerates forward both E_U and E_L exhibit smaller (or even negative) amounts. It is possible that the larger shear strains in the shallower backfill lead to dilation and neither part of the backfill is at a failure state. As the wall accelerates backwards (B to C), E_U and E_L increase and at some moment (point C) at which the wall reaches a maximum backward acceleration, a collision happens between the wall and the backfill and E_U and E_L reach their maximum values. In this case, the dynamic lateral earth pressure at E_U is larger than that at E_L likely because of the larger collision and backward acceleration of the upper elevations of the wall. From point C to D, as the backward acceleration of the wall decreases, E_U and E_L also reduce.

At greater wall acceleration (0.420g in Figure 7), E_U and E_L vary out-of-phase with respect to each other at which E_L fluctuates in-phase and E_U varies out-of-phase with wall acceleration. While the wall is at its largest forward acceleration (point A), E_U drops to its lowest (negative) value and E_L raises to a maximum. In other words, at upper elevations of the wall, the backfill tends to dilate, transmit less lateral stress, and resists failure by accelerating slower than the wall while at greater depths, backfill soil fails (active condition) because of the more contractive tendency at larger stresses and input acceleration, and accelerates faster than the wall hence transmitted larger lateral stresses. Subsequently, the increased magnitude of shaking increases the soil strain amplitude, and thus the soil moves more than the wall. As a result, in forward direction collision occurs between the backfill soil and the wall, and increases earth pressure. As wall acceleration decreases to zero (point B), both E_U and E_L also become zero. When the wall starts to accelerate backwards (point B to C), E_L and E_U respectively decrease and increase which is likely because the wall accelerates backwards faster than the

backfill at E_U and slower than the backfill at E_L. At point C (where wall has the largest backward acceleration), E_L becomes minimum and E_U reaches a maximum value. As wall acceleration drops to zero again (point C to D), E_U and E_L also decrease and increase to zero, respectively. Figures 2 to 7 further show that in all of the cases there exists a phase difference between wall acceleration and dynamic lateral earth pressures and there is no perfect phase compatibility between them.

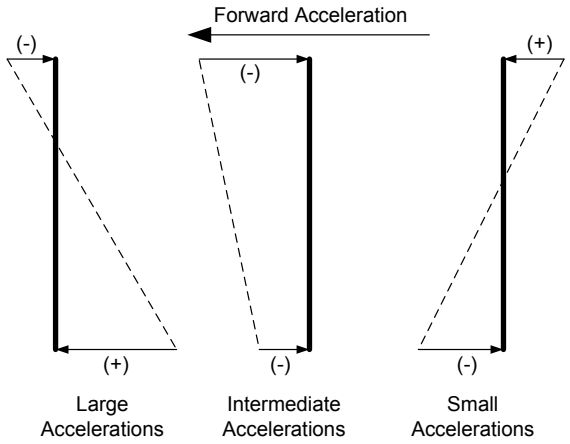

Figure 8a. Schematic distributions of the dynamic lateral pressures when the wall is accelerating forward (away from backfill).

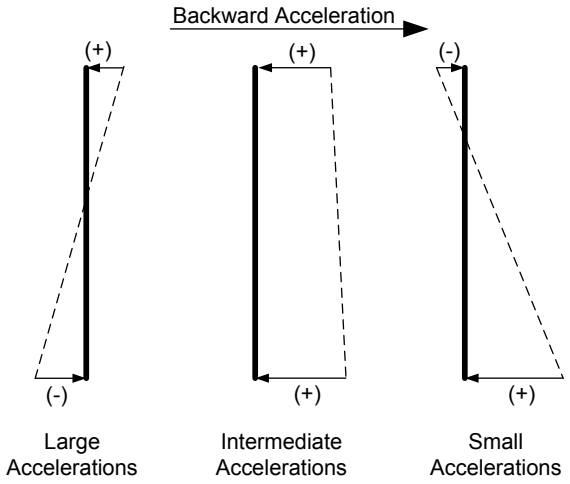

Figure 8b.: Schematic distributions of the dynamic lateral pressures when the wall is accelerating backward (towards backfill).

Figure 8 schematically summarizes the phase relations among the dynamic lateral pressures and wall acceleration observed in Figures 2 to 7. Only at intermediate levels of wall acceleration (0.247g and 0.260g in here) the lateral earth pressures are at similar phases along wall height otherwise at smaller (0.104g, 0.150g, and 0.168g here) and larger (0.420g here) levels of wall acceleration the phases of lateral earth pressures change significantly along wall height and may become out-of-phase. Out of phase acceleration and dynamic lateral earth pressures at intermediate levels of wall acceleration indicates that wall inertia [= -(wall mass)×(wall acceleration)] is in phase with dynamic lateral earth pressures and the wall would move as wall acceleration decreases and earth pressures increase. The in phase variation of dynamic earth pressures and wall displacement with wall inertia force supports the overall validity of using a uniform seismic acceleration coefficient in pseudo-static analysis.

The out of phase fluctuations of dynamic lateral earth pressures on upper and lower elevations of the wall at small and large accelerations, and in phase fluctuations at intermediate accelerations indicates that the wall would tend to rock at small and large accelerations and uniformly oscillate at intermediate wall accelerations. Wall rocking motion can have very detrimental effects on retaining walls and the facilities built on their backfill. For example, the rocking motion of the quay walls narrowed/widened cranes' leg spans during the 1999 Izmit earthquake in Turkey (M_w = 7.4) and led to derailment, tilting and eventually overturning of the cranes (PIANC 2001). Therefore, careful consideration should be given to the rocking motion of walls during earthquakes where conventional design procedures might not be conservative. Note that although the results presented in Figures 2 to 7 and the subsequent interpretations in Figure 8 are limited to dynamic earth pressure measurements at only two elevations of the wall, it is anticipated that similar trends would be observed at other elevations of the wall as well. In addition, although not investigated in this research, it is anticipated that the range of the acceleration amplitudes for small, intermediate, and large levels of shaking would depend on the shear modulus and damping of the soil beneath and behind the wall (which in turn depend on the effective confining pressure and strain level), and inertial and flexural stiffness of the wall as well as and the frequency content of the input motion. The results presented in this paper are obtained with horizontal shaking only and the effect of vertical acceleration is not studied.

4 IMPLICATIONS IN PSEUDO-STATIC ANALYSIS

The very popular pseudo-static method of Mononobe-Okabe (Mononobe and Matsuo 1929; Okabe 1924) assumes that the backfill failure wedge behaves as a perfect plastic rigid body (only the failure plane portion experiences plastic deformation), and the relative displacement between the retaining wall and the retained backfill is negligible and the inertia force acts simultaneously on the retaining wall and the backfill. As a result, amplification of response acceleration, phase lag between the failure wedge and wall acceleration, and non-uniform dynamic soil response within the failure wedge are not considered (Steedman and Zeng 1990; Watanabe et al. 2005; Ghosh 2008) and lateral earth pressures and wall inertia oscillate in-phase with respect to each other. However, as indicated by the model tests of this study, in reality the relative displacement between the retaining wall and the backfill may not be negligible,

and the backfill failure wedge may also deform (i.e. not rigid) as the wall rocks; these invalidate the assumptions of the Mononobe-Okabe method. As observed in this study, depending on the severity of earthquake loading, a uniform peak acceleration may not represent the true seismic response of a retaining wall as the finite shear modulus of the backfill reduces towards the ground surface causing phase change and an amplification of the motion. Consequently, pseudo-static methods would seriously underestimate the amount and distribution of the dynamic lateral earth pressures on a wall. In particular, depending on shaking intensity the resultant thrust point of application on a gravity retaining wall could considerably vary during shaking and the phasing of the maximum and minimum earth pressures could be just the opposite to that estimated from the Mononobe-Okabe approach. According to Figure 8 the point of application of the dynamic lateral thrust would be much higher than that indicated by the Mononobe-Okabe method (assuming a linear dynamic earth pressure distribution) at small (or large) acceleration amplitudes when the wall is moving away from the backfill (or swinging back towards the backfill). Therefore, as indicated by earlier shaking table model studies (e.g., Mononobe and Matsuo 1929; Matsuo 1941; Ishii et al. 1960; Matsuo and Ohara 1960; Seed and Whitman 1970; Richards and Elms 1977; Sheriff et al. 1982; Ortiz et al. 1983; Bolton and Steedman 1985; Andersen et al. 1987; Zeng and Steedman 1988; Steedman and Zeng 1990; Veletsos and Younan 1994; Watanabe et al. 1999; Dakoulas and Gazetas 2008), the Mononobe-Okabe method would give a reasonable estimate of the resultant force as strain localization most likely occurs defining a Coulomb-type active failure wedge (Murphy and Ohara 1960; Bolton and Steedman 1985; Dakoulas and Gazetas 2008), however because of the non-uniform distribution of backfill inertia (as the soil mass of the horizontally moving sliding wedge is largest at the top of the wall and smallest at its base, and so the inertia force on the wedge is concentrated near the top) and thus the variable phasing of the lateral earth pressure components along wall height, the pressure distribution, point of application of the resultant thrust, and the overturning moment may not be correctly estimated. While on the other hand, designing gravity retaining walls for maximum dynamic earth pressure increment and maximum wall inertia (as suggested by Richards and Elms 1977) could be conservative as these values do not fluctuate in-phase with each other, in particular at intermediate wall accelerations at which they fluctuate out-of-phase along the entire height of the wall the maximums of dynamic earth pressures and wall inertia don't occur simultaneously. Accordingly, Al Atik and Sitar (2008) suggest designing retaining walls for dynamic earth pressures corresponding to the maximum dynamic wall moment, rather than for maximum dynamic earth pressures.

5 CONCLUSIONS

Earth retaining structures are complex systems and contact stresses between soil and the structure are the result of the dynamic interaction of the actual system. This study shows that there is always a phase difference between wall acceleration and the dynamic lateral earth pressures on a retaining wall and there is no perfect phase compatibility between them. At some specific range of retaining wall acceleration, the lateral earth pressure distribution and the inertial force applied on the wall would be at similar phases indicating a uniformly oscillating motion of the wall; at this range of wall accelerations, the pseudo-static methods (with uniform seismic acceleration coefficients) can be used to approximately model earthquake loading. However, at accelerations below and above this range, dynamic lateral earth pressures on different levels of the wall may become considerably out-of-phase. This suggests that the wall would rock and the soil within the failure wedge would also deform. Therefore, in addition to the inertia effects (characterized by the Mononobe-Okabe and Westergaard methods), the periodic rotation, tilting, and rocking of the wall also influences the cyclic fluctuations of the effective earth and water pressures and plays a considerable role in the phasing of these pressures during earthquakes. Clearly, the entire problem is very complex and with the present state of knowledge there is no clear understanding of the levels of weak, intermediate, and strong shaking intensities and the effect of soil and wall properties, and ground motion characteristics (frequency content, vertical acceleration, and duration) on these levels is to be further studied.

Such phase lags between the lateral soil pressures and acceleration of the wall, and the non-uniform response inside the backfill soil are likely because of the relative displacements between the retaining wall and the backfill soil and the subsequent collision or lagging of the wall and the backfill. In fact, the phase change causes the point of application of the resultant thrust to be above the 1/3 of wall height. These experimental observations are in contrast to the common assumptions made in pseudo-static analysis i.e. rigid body deformation of the backfill failure wedge and negligible relative displacement between the retaining wall and the retained backfill soil and the subsequent assumption of simultaneous occurrence of maximum earth pressure and inertia force. Therefore, using a uniform acceleration over the entire height of a wall in pseudo-static analysis does not reflect the actual seismic behaviour and this approach could underestimate the actual resultant thrust and overturning moment on a wall leading to an unsafe design. Whereas, designing retaining walls for maximum dynamic earth pressures and maximum wall inertia does not reflect the true seismic behaviour of a wall and would be very conservative as these maximums don't occur at the same time.

REFERENCES

AASHTO 2006. Recommended LRFD guidelines for the seismic design of highway bridges. American Association of State Highway and Transportation Officials (AASHTO), National Cooperative Highway Research Program (NCHRP), Transportation Research Board.

Al Atik, L. and Sitar, N. 2008. Experimental and analytical study of the seismic performance of retaining structures. Pacific Earthquake Engineering Report, Report 2008/104, University of California, Berkeley.

Andersen, G. R., Whitman, R. V. and Germaine, J. T. 1987. Tilting response of centrifuge-modeled gravity retaining wall to seismic shaking. Report No. R87-14, Department of the Civil Engineering, Massachusetts Institute of Technology, Cambridge, MA., USA, 1987.

ASCE 4-98 2000. Seismic analysis of safety related nuclear structures and commentary. American Society of Civil Engineers.

Bolton M. D., and Steedman, R. S. 1985. The behavior of fixed cantilever walls subject to lateral loading. Application of Centrifuge Modeling to Geotechnical Design, Craig (ed.), Balkema, Rotterdam.

CHBDC 1998. Canadian Highway Bridge Design Code. Canadian Standards Association.

Choudhury, D. and Ahmad, S. M. 2008. Stability of waterfront retaining wall subjected to pseudodynamic earthquake forces. Journal of Waterway, Port, Coastal, and Ocean Engineering, 134(4): 252 – 260.

Choudhury, D. and Singh, S. 2006. New approach for estimation of static and seismic active earth pressure. Geotechnical and Geological Engineering, 24(1): 117-127.

Coe, C. J., Prevost, J. H. and Scanlan, R. H. 1985. Dynamic stress wave reflection/attenuation: earthquake simulation in centrifuge soil models. Journal of Earthquake Engineering and Soil Dynamics, 13: 109-128.

COSMOS 2010. Consortium of Organizations for Strong-Motion Observation Systems. Strong Motion Data Center <db.cosmos-eq.org/scripts/default.plx>.

Dakoulas, P. and Gazetas, G. 2008. Insight into seismic earth and water pressures against caisson quay walls. Geotechnique, 58(2): 95 – 111.

Dewoolkar, M. M., Ko, H.-Y., and Pak, R. Y. S. 2001. Seismic behavior of cantilever retaining walls with liquefiable backfills. Journal of Geotechnical and Geoenvironmental Engineering, 127(5): 424-435.

EAU 1996. Recommendations of the Committee for Waterfront Structures, Harbours, and Waterways. 7th Edition, 2000, Ernst & Sohn.

Ebeling, R. M., Morrison, E. E., Whitman, R. V., and Liam Finn, W. D. 1992. A manual for seismic design of waterfront retaining structures. US Army Corps of Engineers, Technical Report ITL-92-11.

EN 1997, 2002. Eurocode 7 Geotechnical Design - Part 1: General Rules. CEN European Committee for Standardization, Bruxelles, Belgium.

FEMA 369, 2000. The 2000 NEHRP Recommended Provisions for New Buildings and Other Structures. Part 2: Commentary. Federal Emergency Management Agency.

FHWA 1997. Geotechnical Engineering Ciruclar #3. Design Guidance: Geotechnical Earthquake Engineering for Highways, Design Principles. FHWA-SA-97-076, Federal Highway Administration, Vol. I, U.S. Department of Transportation.

Ghosh, P. 2008. Seismic active earth pressure behind a nonvertical retaining wall using pseudo-dynamic analysis. Canadian Geotechnical Journal, Technical Note, 45(1):117-123.

IBC (International Building Code) 2006. Country Club Hills, IL : International Code Council, 664 pp.

Ishii, Y., Arai, H. and Tsuchida, H. 1960. Lateral earth pressure in an earthquake. *In* Proceedings of the 2nd World Conference on Earthquake Engineering, Tokyo, pp. 211-230.

Kazama, M. and Inatomi, T. 1993. Dynamic earth pressure and dynamic water pressure of fills behind quaywalls. Engineered Fills, Edited by B.G. Clarke, C.J.F.P. Jones, & A.I.B. Moffat: 140-152.

Kim, S. –R., Kwon, O., -S., and Kim, M. –M. 2004. Evaluation of force components acting on gravity type quay walls during earthquakes. Soil Dynamics and Earthquake Engineering, 24: 853 – 866.

Lacasse, S. and Berre, T. 1988. State-of-the-Art Paper: triaxial testing methods for soils. *In Advanced Triaxial Testing of Soil and Rock*, Robert T. Donaghe, Ronald C. Chaney, and Marshall L. Silver (eds.), STP 977: 264 – 289.

Ladd, R. S. 1978. Preparing test specimens using undercompaction. Geotechnical Testing Journal, ASTM, 1: 16 – 23.

Lee, C. J. 2005. Centrifuge modeling of the behavior of caisson-type quay walls during earthquakes. Soil Dynamics and Earthquake Engineering, 25(2): 117 – 131.

Mandrescu, N., Radulian, M., and Marmureanu, G. (2002). “Site conditions and predominant period of seismic motion in the Bucharest urban area.” International Symposium, 25 Years of Research in Earth Physics and Once Century of Seismology in Romania, 27-29 September, Bucharest, Romania.

Matsuo, H. 1941. Experimental study on the distribution of earth pressures acting on a vertical wall during earthquakes. Journal of the Japanese Society of Civil Engineers, 27(2).

Matsuo, H. and Ohara, S. 1960. Lateral earth pressure and stability of quay walls during earthquakes. *In* Proc. 2nd World Conference on Earthquake Engineering.

Mononobe, N. and Matsuo, M. 1929. On the determination of earth pressures during earthquakes. *In* Proceedings of World Engineering Congress, Vol. 9, pp. 177-185.

Murphy, H. and Ohara, S. 1960. Lateral earth pressure and stability of quay walls during earthquakes. *In* Proc. 2nd World Conference on Earthquake Engineering, Tokyo, pp. 165 – 187.

Mylonakis, G., Kloukinas, P., and Papantonopoulos, C. 2007. An alternative to the Mononobe-Okabe equations for seismic earth pressures. Soil Dynamics and Earthquake Engineering, 27: 957-969.

Nakamura, S. 2006. Reexamination of Mononobe-Okabe theory of gravity retaining walls using centrifuge model tests. Soils and Foundations, 46: 135 – 146.

Okabe, S. 1924. General theory of earth pressure and seismic stability of retaining wall and dam. Journal of the Japanese Society of Civil Engineers, 10(5): 1277-1323.

Ortiz, L. A., Scott, R. F. and Lee, J. 1983, Dynamic centrifuge testing of a cantilever retaining

wall. Earthquake Engineering and Structural Dynamics, 11(2): 251 - 268.

PIANC 2001. Seismic design guidelines for port structures. International Navigation Institute, Tokyo: A. A. Balkema Publishers.

Pitilakis, K. and Moutsakis, A. 1989. Seismic analysis and behavior of gravity retaining walls – the case of Kalamata harbor quaywall. Soils and Foundations, Japanese Society of Soil Mechanics and Foundation Engineering, 29(1): 1- 17.

Richards, Jr. R., and Elms, D. 1977. Seismic behavior of gravity retaining walls. Research report No. 77-10. University of Canterbury, Christchurch, New Zealand.

Richards, R., Huang, C., and Fishman, K. L. 1999. Seismic earth pressure on retaining structures. Journal of Geotechnical and Geoenvironmental Engineering, ASCE, 125(9): 771-778.

Sadrekarimi, A. 2004. Seismic performance of gravity quay walls. M.Sc. Thesis, University of Tehran, Iran.

Seed, H. B. and Whitman, R. V. 1970. Design of earth retaining structures for dynamic loads. *In* Proceedings, ASCE Specialty Conference on Lateral Stresses in the Ground and Design of Earth Retaining Structures, pp. 103-147.

Sherif, M. A. and Fang, Y. S. 1984a. Dynamic earth pressure on walls rotating about top. Soils and Foundations, 24(4): 109-117.

Sherif, M. A. and Fang, Y. S. 1984b. Dynamic earth pressures on rigid walls rotating about the base. Proc. of 8th World Conference on Earthquake Engineering, San Francisco, USA, Vol. 6, pp. 993 - 1000.

Sherif, M. A., Ishibashi, I. and Lee C. D. 1982. Earth pressures against rigid retaining walls. Journal of Geotechnical Engineering, 108(GT5): 679-696.

Steedman, R. S. and Zeng, X. 1990. The influence of phase on the calculation of pseudo-static earth pressure on a retaining wall. Geotechnique, 40:103-112.

Tajimi H. 1973. Dynamic earth pressure on basement wall. *In* Proc. 5th World Conf. Earthquake Eng., Rome, 2, pp. 1560 – 1569.

Ting, N. -H. 1993. Earthquake-induced tilt of retaining wall with saturated backfill. Ph.D. thesis, Department of Civil and Environmental Engineering, Massachusetts Institute of Technology.

Veletsos A. S. and Younan, A. H. 1994. Dynamic soil pressures on rigid retaining walls. Earthquake Engineering Structural Dynamics, 23: 275-301.

Watanabe, K., Koseki, J., and Tateyama, M. 2005. Application of high-speed digital CCD cameras to observe static and dynamic deformation characteristics of sand. Geotechnical Testing Journal, 28(5): 1 – 13.

Watanabe, K., Maeda, T., Kobayashi, Y., and Towhata, I. 1999. Shaking table tests on seismic earth pressure exerted on retaining wall model. *Proceedings of the Second International Conference on Earthquake Geotechnical Engineering*, Pedro S. Seco e Pinto, Ed., Balkema, Lisbon, Vol.1: 297-302.

Whitman, R. V. 1990. Seismic design and behavior of gravity retaining walls. *In* Proc. Conf. on Design and Performance of Earth Retaining Structures, ASCE Geotechnical Special Publication, 25: 817 – 842.

Wood, J. H. 1973. Earthquake induced soil pressures on structures. Doctoral Dissertation, EERL 73-50, Pasadena, CA: California Institute of Technology.

Zeng, X. 1998. Seismic response of gravity quay walls. I: centrifuge modeling. Journal of Geotechnical and Geoenvironmental Engineering, 124(5): 406-417.

Zeng, X. and Steedman R. S. 1988. Seismic Design of Retaining Walls, Research Report No. R88-07, Department of Civil Engineering, MIT.

Zeng, X. and Steedman, R. S. 1993. On the behaviour of quay walls in earthquakes. Geotechnique, 43(3): 417 – 431.